

Antitumor mechanisms of combined gastrin-releasing peptide receptor and epidermal growth factor receptor targeting in head and neck cancer

Qing Zhang,² Neil E. Bhola,² Vivian Wai Yan Lui,⁶ Doris R. Siwak,⁴ Sufi M. Thomas,¹ Christopher T. Gubish,² Jill M. Siegfried,^{2,3} Gordon B. Mills,⁴ Dong Shin,⁵ and Jennifer Rubin Grandis^{1,2,3}

Departments of ¹Otolaryngology and ²Pharmacology, University of Pittsburgh School of Medicine and ³University of Pittsburgh Cancer Institute, Pittsburgh, Pennsylvania; ⁴Department of Molecular Therapeutics, University of Texas M. D. Anderson Cancer Center, Houston, Texas; ⁵Department of Medicine, Emory University, Atlanta, Georgia; and ⁶Department of Clinical Oncology, The Chinese University of Hong Kong, Hong Kong

Abstract

Head and neck squamous cell carcinoma (HNSCC) is characterized by epidermal growth factor receptor (EGFR) overexpression, where EGFR levels correlate with survival. To date, EGFR targeting has shown limited antitumor effects in head and neck cancer when administered as monotherapy. We previously identified a gastrin-releasing peptide/gastrin-releasing peptide receptor (GRP/GRPR) autocrine regulatory pathway in HNSCC, where GRP stimulates Src-dependent cleavage of EGFR proligands with subsequent EGFR phosphorylation and mitogen-activated protein kinase (MAPK) activation. To determine whether GRPR targeting can enhance the antitumor efficacy of EGFR inhibition, we investigated the effects of a GRPR antagonist (PD176252) in conjunction with an EGFR tyrosine kinase inhibitor (erlotinib). Combined blockade of GRPR and EGFR pathways significantly inhibited HNSCC, but not immortalized mucosal epithelial cell, proliferation, invasion, and colony formation. In addition, the percentage of apoptotic cells increased upon combined inhibition. The enhanced antitumor efficacy was accompanied by increased expression of cleaved poly(ADP-ribose) polymerase (PARP) and decreased phospho-EGFR, phospho-MAPK, and proliferating cell nuclear antigen (PCNA). Using reverse-phase protein microarray

(RPPA), we further detected decreased expression of phospho-c-Jun, phospho-p70S6K, and phospho-p38 with combined targeting. Cumulatively, these results suggest that GRPR targeting can enhance the antitumor effects of EGFR inhibitors in head and neck cancer. [Mol Cancer Ther 2007;6(4):1414–24]

Introduction

Head and neck squamous cell carcinoma (HNSCC) accounts for 90% of head and neck cancers (1). HNSCC is the sixth most common cancer worldwide, with ~40,000 new cases and 12,000 deaths annually in the United States (2). The major risk factors for the development of HNSCC include tobacco usage and alcohol consumption. Standard treatment for head and neck cancer includes surgery followed by chemoradiation or chemoradiation alone. Despite a nearly 60% 5-year survival rate for primary HNSCC, most HNSCC patients die of a secondary aerodigestive tract cancer. The survival from secondary primary tumors remains below 25%; there has been little evidence of an improvement in the 5-year survival rate over the past several decades (3, 4). Although the critical pathways that contribute to HNSCC formation remain largely unknown, the epidermal growth factor receptor (EGFR) has been implicated in HNSCC development and progression. Approximately 95% of HNSCC tumors over-express EGFR when compared with levels in normal mucosa (5).

Elevation of EGFR in HNSCC is accompanied by increased expression of its ligand, transforming growth factor α (TGF- α) supporting an autocrine regulatory pathway in this tumor system. In HNSCC tumors, the expression level of EGFR in the tumor predicts decreased survival, independent of nodal status (N stage; ref. 5). Abrogation of EGFR *in vitro* or *in vivo* inhibits HNSCC proliferation without affecting the growth of normal mucosal epithelial cells (5–7). The critical importance of EGFR in HNSCC is shown by the remarkable results of phase I clinical trials where treatment with a monoclonal antibody (C225) directed against EGFR in combination with either cisplatin or radiotherapy resulted in a response rate of nearly 100% (8, 9). However, targeting EGFR with either tyrosine kinase inhibitors or monoclonal antibodies has shown limited antitumor effects in head and neck cancer patients when these agents are delivered as monotherapy (10, 11). A phase II clinical trial with the EGFR tyrosine kinase inhibitor erlotinib reported only a 5% response rate in 115 head and neck cancer patients (12).

The constitutive activation of G-protein-coupled receptors (GPCR) leading to the transactivation of EGFR and other signaling pathways may contribute to the low

Received 11/3/06; revised 1/22/07; accepted 2/19/07.

Grant support: NIH grants R01 CA098372-01 (J.R. Grandis), P50 CA097190-01A1 (J.R. Grandis), and U01 CA101244 (D. Shin).

The costs of publication of this article were defrayed in part by the payment of page charges. This article must therefore be hereby marked *advertisement* in accordance with 18 U.S.C. Section 1734 solely to indicate this fact.

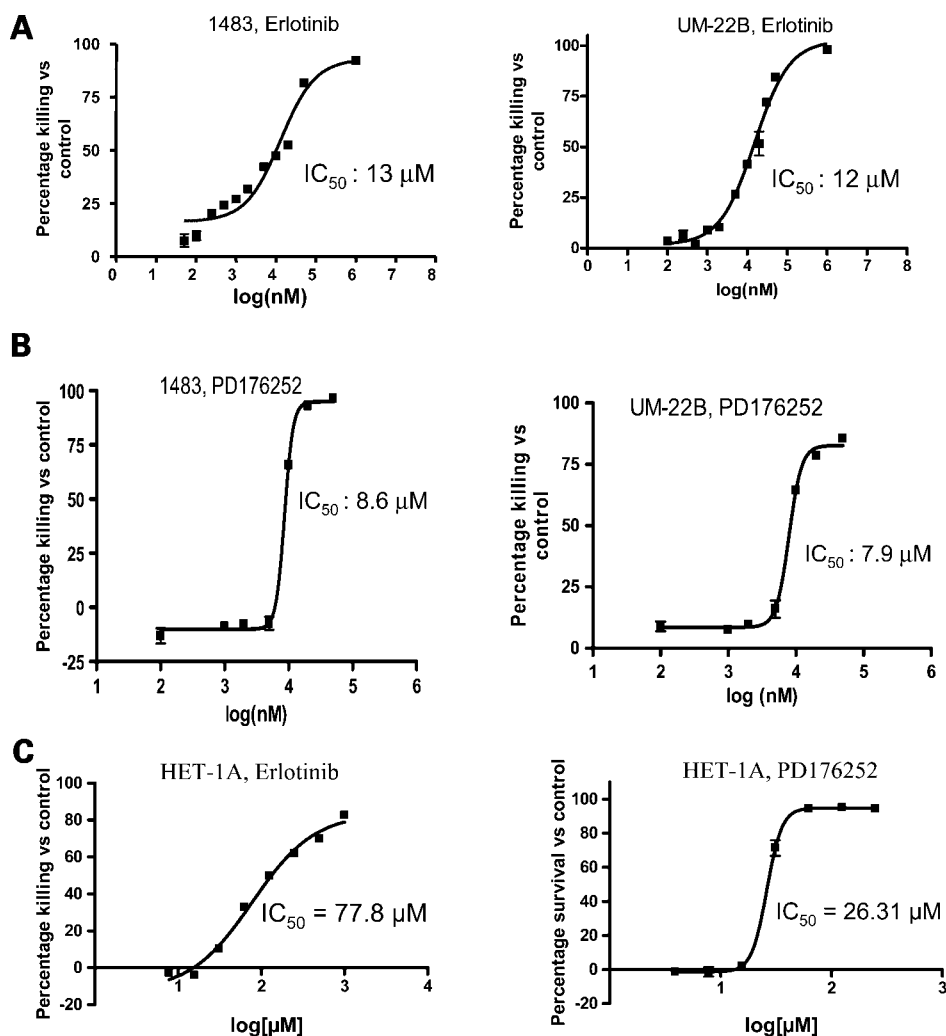
Requests for reprints: Jennifer Rubin Grandis, Room 105, The Eye and Ear Institute, 200 Lothrop Street, Pittsburgh, PA 15213.

Phone: 412-647-5280; Fax: 412-647-0108. E-mail: jgrandis@pitt.edu

Copyright © 2007 American Association for Cancer Research.

doi:10.1158/1535-7163.MCT-06-0678

Figure 1. Dose response growth inhibition using erlotinib and PD176252. HNSCC cells (1483, UM-22B) were treated with (A) erlotinib or (B) PD176252, followed by MTT assay 3 d later. C, the growth inhibitor effects of erlotinib and PD176252 were also examined in HET-1A cells. The data were analyzed using Prism (GraphPad Software) to determine the IC_{50} dose of both drugs. The experiment was repeated thrice with similar results.



response rate in head and neck cancer receiving EGFR targeting therapy (13–15). We previously reported that the gastrin-releasing peptide (GRP) induces EGFR activation and downstream mitogen-activated protein kinase (MAPK) phosphorylation, which potentiates head and neck cancer cell invasion and proliferation (16). In addition, the gastrin-releasing peptide receptor (GRPR) is overexpressed in both HNSCC tumors and adjacent normal mucosa from HNSCC patients compared with levels in control mucosa from individuals without cancer where increased GRPR levels were associated with decreased survival (17). These results suggest that the constitutive activation of downstream signaling pathways by GRPR may contribute to the resistance to EGFR inhibitors in HNSCC.

Integration of GRPR and EGFR signaling in cancer cells indicates that treatment regimens designed to target both receptor pathways may be efficacious. To determine whether the addition of GRPR targeting can enhance the antitumor efficacy of EGFR tyrosine kinase inhibitors, the GRPR antagonist PD176252 was combined with the EGFR tyrosine kinase inhibitor erlotinib in HNSCC cell lines and

immortalized mucosal epithelial cells (18). To explore the potential mechanisms of combined targeting of GRPR and EGFR and identify intermediate biomarkers of therapeutic efficacy, we examined total protein and phosphoprotein levels of downstream signaling molecules using reverse-phase protein microarray (RPPA) and Western blotting. We found that in addition to predicted proteins based on known mechanisms, phospho-c-Jun, phospho-p70S6K, and phospho-p38 levels were further decreased by combined targeting of GRPR and EGFR when compared with EGFR inhibition alone. These results suggest that the addition of a GRPR inhibitor can block both EGFR-dependent as well as EGFR-independent pathways leading to enhanced antitumor effects.

Materials and Methods

Chemicals and Reagents

The EGFR monoclonal antibody used for Western blotting was obtained from BD Transduction (San Jose, CA). The EGFR antibody for immunoprecipitation was

obtained from Upstate Biotechnology (Lake Placid, NY). PD176252 (18) was obtained from Pfizer Parke-Davis (Ann Arbor, MI). β -Actin antibody was obtained from EMD Biosciences (San Diego, CA). Erlotinib was a kind gift from OSI Pharmaceutical Company (Melville, NY; ref. 19). Antibodies against p44/42 MAPK, phospho-p44/42 MAPK, cleaved PARP, Akt, and phospho-Akt (Ser⁴⁷³) were obtained from New England Biolabs (Beverly, MA). The proliferating cell nuclear antigen (PCNA) antibody was from Santa Cruz Biotechnology (Santa Cruz, CA).

Cell Culture

HNSCC cell lines (1483 and UM-22B) were of human origin and derived from an oropharyngeal tumor and metastatic cervical lymph node as described previously (20, 21). Cells were maintained in DMEM with 12% heat-inactivated FCS (Invitrogen, Carlsbad, CA) at 37°C with 5% CO₂. The 1483 cell line was derived from an oropharyngeal tumor, and the UM-22B cell line was derived from a metastatic cervical lymph node. HET-1A cells were purchased from the American Type Culture Collection (Manassas, VA). The HET-1A cells are normal human esophageal mucosa cells immortalized by transfection with the SV40 large T antigen as described previously (22).

Western Blotting

Approximately 25 μ g of protein was resolved in an 8% SDS-PAGE gel and transferred onto a Protran membrane (Schleicher & Schuell Inc., Keene, NH) using a semidry transfer machine (Bio-Rad Laboratories, Hercules, CA). After protein transfer, the membrane was blocked

overnight with a blocking solution containing 5% nonfat dry milk, 0.2% Tween 20 in 1 \times PBS. The membrane was incubated with the primary antibodies (1:1,000 phospho-p44/42 MAPK or p44/42 MAPK, PCNA, cleaved PARP, phospho-Akt473, total Akt, and β -actin) for 2 h and then washed with Blotto solution [0.6% dry milk powder, 0.9% NaCl, 0.5% Tween 20, and 50 mmol/L Tris (pH 7.4)] thrice for 10 min. The membrane was then incubated with the secondary antibody (goat anti-rabbit/mouse immunoglobulin G-horseradish peroxidase conjugate; Bio-Rad) for 1 h and washed thrice for 10 min. The membrane was quickly rinsed with a rinsing solution [0.1% Tween 20, 100 mmol/L Tris (pH 8.0), and 150 mmol/L NaCl], and the blot was developed with luminol reagent (Santa Cruz Biotechnology). The band intensity was quantitated with DigiDoc1000 software (Alpha Innatech Corporation, San Leandro, CA) as described previously (23).

Matrigel Invasion Assay

Cell invasion was evaluated *in vitro* using Matrigel-coated semipermeable modified Boyden inserts with a pore size of 8 μ m (Becton Dickinson/Biocoat, Bedford, MA). Cells were plated in duplicate at a density of 4 \times 10⁴ cells per well in DMEM in the chamber or insert. Both the insert and the holding well were subjected to the same medium composition with the exception of serum. The insert contained no serum, whereas the lower well contained 10% fetal bovine serum (FBS) that served as a chemo-attractant. The lower wells were supplemented with DMSO, PD176252 (4 μ mol/L), erlotinib (6 μ mol/L), or a

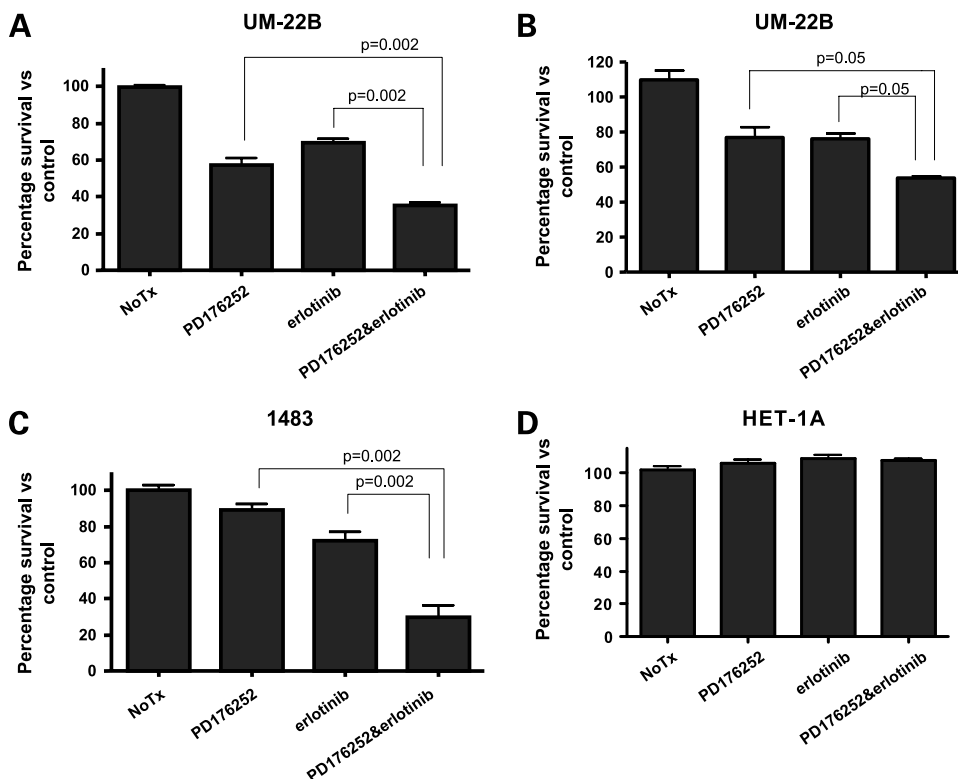


Figure 2. Combination of GRPR and EGFR targeting enhances growth inhibition. HNSCC cells UM-22B (A), 1483 (C), or HET-1A (D) cells were plated on 24-well plates, followed by treatment with PD176252 (4 μ mol/L), erlotinib (6 μ mol/L), or PD176252 (4 μ mol/L) + erlotinib (6 μ mol/L) in triplicate. B, in addition, UM-22B cells were treated with lower doses of PD176252 (2 μ mol/L) and erlotinib (2 μ mol/L) alone and in combination. MTT assay was done 3 d later. The percentage of cell survival was calculated according to the equation of $OD_{drug}/OD_{vehicle} \times 100\%$. Experiments in A, C and D were repeated six times, and the experiments in B were repeated thrice with similar results. P values were determined by comparing combined treatment to PD176252 or erlotinib treatment alone ($P = 0.002$ for A and C; $P = 0.05$ for B).

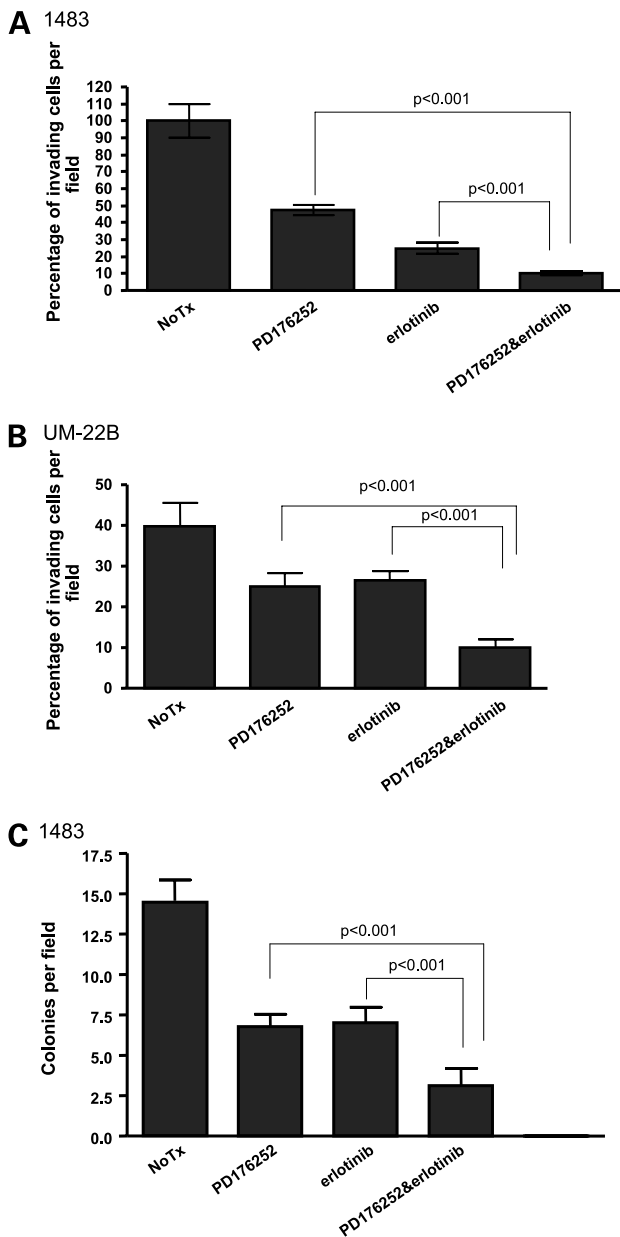


Figure 3. Combined inhibition of GRPR and EGFR decreases HNSCC cell invasion and colony formation. **A** and **B**, 1483 and UM-22B cells were plated in Matrigel invasion chamber in triplicates followed by treatment with PD176252 (4 $\mu\text{mol/L}$), erlotinib (6 $\mu\text{mol/L}$), or a combination of PD176252 and erlotinib for 24 h. Invading cells in four representative fields were counted using light microscopy at $\times 400$ magnification. Columns, mean calculated from two independent experiments; bars, SE. *P* values were determined by comparing combined treatment to PD176252 or erlotinib treatment alone ($P < 0.001$). **C**, 1483 cells were plated on 60-mm culture plates that were covered with a layer of 0.5% agar in medium supplemented with 20% FBS in combination with PD176252 (4 $\mu\text{mol/L}$), erlotinib (6 $\mu\text{mol/L}$), or a combination of PD176252 and erlotinib. Cell suspensions (500 cells per well) were prepared in 0.3% agar and poured into 60-mm culture plates. The plates were incubated at 37°C in a humid atmosphere of 5% CO_2 for 2 wks until colonies appeared. The colonies were stained with MTT (1–2 mg/mL). Ten different fields were counted by light microscopy for each treatment ($P < 0.001$). All experiments were repeated twice with similar results.

combination of PD176252 and erlotinib. After 48 h of treatment at 37°C in a 5% CO_2 incubator, the cells in the insert were removed by wiping gently with a cotton swab. Cells on the reverse side of the insert were fixed and

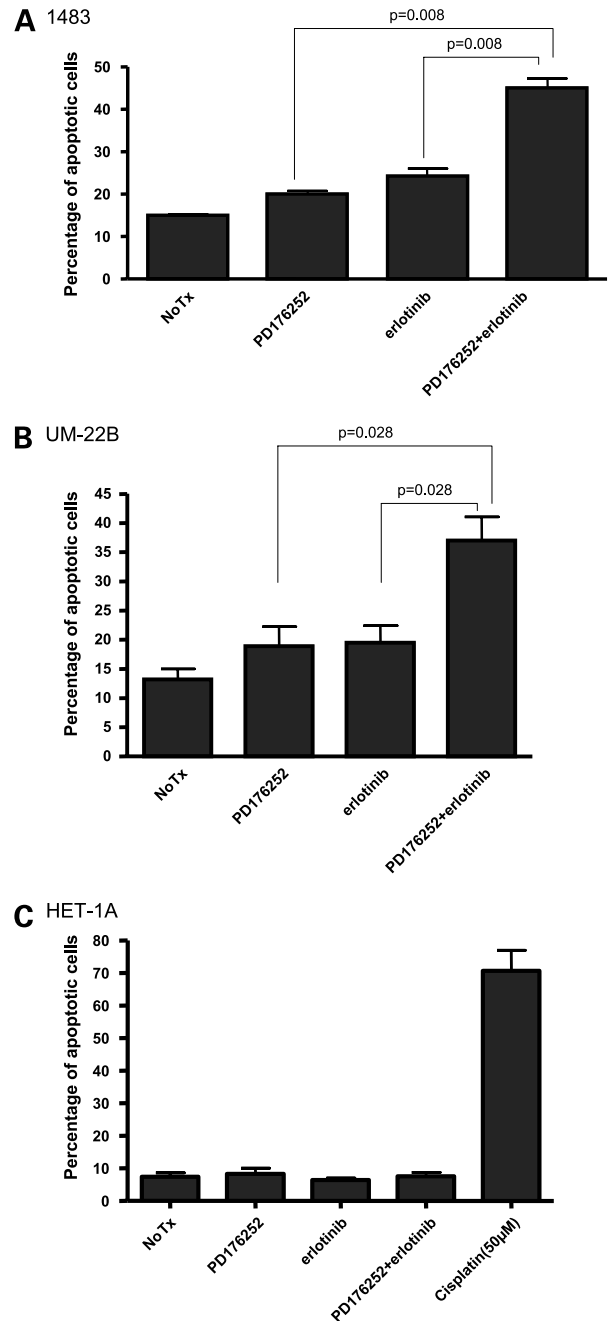


Figure 4. Combined targeting of GRPR and EGFR increases HNSCC apoptosis. 1483 (**A**), UM-22B (**B**), or HET-1A (**C**) cells were treated with PD176252 (4 $\mu\text{mol/L}$), erlotinib (6 $\mu\text{mol/L}$), or a combination of PD176252 and erlotinib for 24 h followed by annexin-V assay. *P* values were determined by comparing PD176252 + erlotinib treatment to single drug treatment. The experiments in **A** and **C** were done five times, and the experiments in **B** were repeated 4 times with similar results (**A**, $P = 0.008$; **C**, $P = 0.028$).

stained with Hema 3 (Fisher Scientific, Hampton, NH) according to the manufacturer's instructions. Invading cells in four representative fields were counted using light microscopy at 400× magnification. Mean ± SE was calculated from independent experiments.

In vitro Apoptosis Assay

After treating HNSCC and HET-1A cells with PD176252, erlotinib or PD176252+ erlotinib, cells were detached by trypsinization, counted, and pelleted (1,000 rpm for 5 min). Cell pellets were washed once with PBS (pH 7.4) and resuspended in 100 μL annexin V binding buffer [10 mmol/L HEPES (pH 7.4), 140 mmol/L NaCl, 2.5 mmol/L CaCl₂]. About 5 μL of annexin V-Cy3 (BioVision Research Products, Mountain View, CA) was added per tube and allowed to incubate at room temperature for 15 min in the dark. Then, the stained cell suspension was dropped on the slides and covered with coverslips. The membrane of apoptotic cells is stained a bright orange color when analyzed with fluorescence microscopy. The ratio (percentage) of apoptotic to total cells (apoptotic plus nonapoptotic cells) was calculated for each high-power field. For each treatment, 5 to 10 high-power fields of view were quantitated on each section.

Cell Survival Analysis

HNSCC or HET-1A cells were plated at 4×10^4 cells per well in 24-well plates. After treating cells with PD176252, erlotinib, or PD176252 + erlotinib for 72 h, 3-(4,5-dimethylthiazol-2-yl)-2,5-diphenyltetrazolium bromide (MTT) assay was done to determine the cytotoxic effects of drug treatment. Percentage of cell survival was determined by comparing drug treatment to vehicle. The equation used to calculate the survival percentage is $OD_{drug}/OD_{vehicle} \times 100\%$.

Colony Formation Assay

Culture plates (60 mm) were covered with a layer of 0.5% agar in medium supplemented with 20% FBS in combination with PD176252, erlotinib, or PD176252 + erlotinib. Cell suspensions (500 cells per well) were prepared in 0.3% agar and poured into 60-mm culture plates. The plates were incubated at 37°C in a humid atmosphere of 5% CO₂ for 2 weeks until colonies appeared. The colonies were stained with MTT (1–2 mg/mL) and counted.

Cell Cycle Analysis

The 1483 and UM-22B cells were treated with PD176252 or erlotinib alone or with a combination of PD176252 and erlotinib for 24 h. Cells were fixed by 75% ethanol followed by propidium iodide (5 μg/mL) and RNase A (10 μg/mL) and then analyzed by flow cytometry (Epics XL-MCL; Beckman Coulter, Miami, FL).

RPPA Sample Preparation

Cells were plated on a 10-cm plate. After treatment, cells were washed twice with ice cold PBS. Then, lysis buffer [1% Triton X-100, 50 mmol/L HEPES (pH 7.4), 150 mmol/L NaCl, 1.5 mmol/L MgCl₂, 1 mmol/L EGTA, 100 mmol/L NaF, 10 mmol/L NaPPi, 10% glycerol, 1 mmol/L phenylmethylsulfonyl fluoride, 1 mmol/L Na₃VO₄, and 10 μg/mL aprotinin] was added to the cells followed by microcentrifugation at 14,000 rpm for 10 min. Clear supernatants were accumulated followed by protein quantitation using the protein assay solution (Bio-Rad) and bovine serum albumin of known concentration as the standard. The cell lysate was mixed with 4× SDS sample buffer without bromophenol blue [three parts of cell lysate plus one part of 4× SDS sample buffer, which contained 35% glycerol, 8% SDS, 0.25 mol/L Tris-HCl (pH 6.8)]. Before use, 10% β-mercaptoethanol was added. The samples were boiled for 5 min. Then, samples were serially diluted (1:2–1:128). To each of the diluted samples, an equal amount of 80% glycerol/2× PBS solution was added, followed by a transfer of the diluted samples to 384-well plates. Lysates were arrayed by a pin and ring GMSE 417 arrayer (Affymetrix, Santa Clara, CA) onto nitrocellulose slides.

RPPA Staining

Slides were washed with reblot buffer (Chemicon, Temecula, CA) for 15 min followed by two washes with PBS. Then array slides were blocked with I-block (Applied Biosystems, Bedford, MA) for 30 min. Hydrogen peroxide was applied on the slides for 5 min, followed by washes with TBST for 5 min. Avidin and biotin were applied on the slides for 5 min followed by TBST washes. After that, six to seven drops of protein block were added onto each slide followed by antibody incubation at RT for 1 h. After two washes with TBST, biotin-conjugated secondary antibody was applied on the slides for 30 min followed by washes with TBST. Streptavidin-biotin complex was then used to cover the slides for 15 min. Finally, amplification reagents were applied on the slides followed by streptavidin peroxidase (15 min) and substrate-chromogen incubation (5 min). Stained slides were scanned and analyzed by microvigen software. The c-jun-NH₂-kinase (JNK) antibody was purchased from Santa Cruz Biotechnology (1: 750). The remaining antibodies were purchased from Cell Signaling Technology (Beverly, MA) and used at the following dilutions: phospho-c-Jun p73 (1:100), phospho-p70S6K (1:250),

Table 1. Cell cycle analysis upon GRPR/EGFR inhibitor treatment

Cell line	Phase	Control	PD176252	Erlotinib	PD176252 + erlotinib ($P_{1,2}$)*
1483	G ₀ -G ₁	39.2	49.8	44.9	61.6 ($P_1 = 0.028$; $P_2 = 0.028$)
	S	29.8	27.4	29.2	21.5 ($P_1 = 0.028$; $P_2 = 0.028$)
	G ₂ -M	26.4	18.7	22.0	14.2

* P value was determined for comparison of G₀-G₁, S or G₂-M cell population in PD176252 (P_1) or (P_2) with that in the combined treatment by Wilcoxon test from four independent (1483) experiments, and multiple comparisons within the same experiment were adjusted with the Bonferroni procedure.

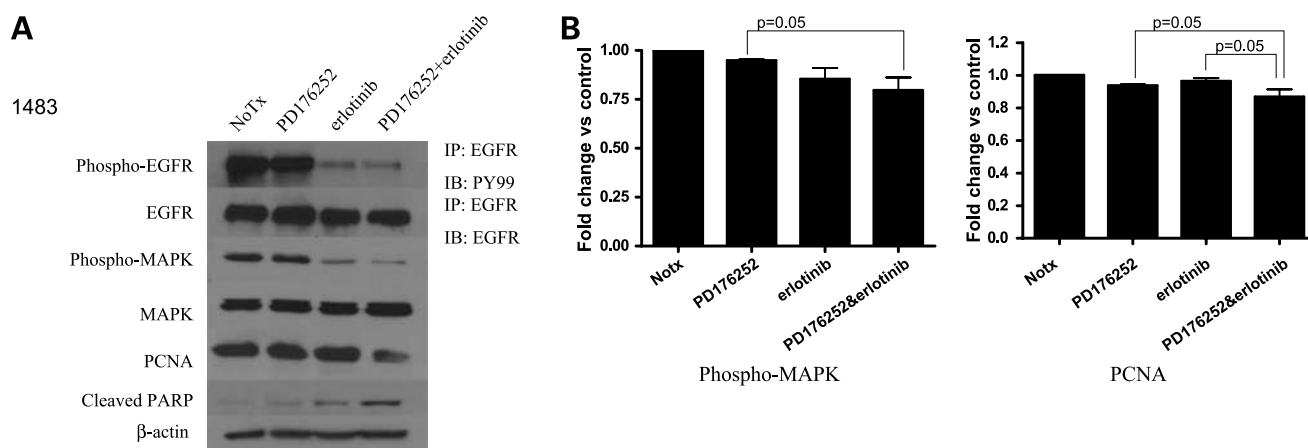


Figure 5. Combination therapy targeting GRPR and EGFR modulates cell signaling pathways. **A**, HNSCC cells (1483) were treated with PD176252 (4 $\mu\text{mol/L}$), erlotinib (6 $\mu\text{mol/L}$), or a combination of PD176252 and erlotinib for 48 h, followed by Western blotting or immunoprecipitation as indicated for phospho-EGFR, phospho-MAPK ($P = 0.038$, combined treatment compared with erlotinib treatment alone), PCNA ($P = 0.0248$, combined treatment compared with PD176252 treatment alone), cleaved PARP ($P = 0.0248$, combined treatment compared with either treatment alone), and β -actin. **B**, bar graphs represent the cumulative results of three independent experiments.

phospho-p38 (1:200), phospho-Rb (Ser^{807/811}; 1:250), phospho-Akt (Ser⁴⁷³; 1:200), and p38 (1:300). To quantify the individual samples, microvigene software (VigeneTech, Inc) was used. The serial dilution “dot” intensities for each sample were quantitated and converted to a single value, the dilution intensity 30 (DI₃₀ value, obtained from the intensity log₂-dilution curve). The DI₃₀ value for each sample stained with a particular antibody (e.g., EGFR antibody) represents the corresponding amount of the target protein, EGFR, in the sample. To correct for the possible loading error (similar to loading correction in a Western blotting analysis), the DI₃₀ values were normalized to a sample conversion factor. The sample conversion factor is based on several proteins with relatively unchanged levels in the RPPA. These included JNK, p38, and Akt, which served as loading controls for RPPA staining.

Statistics

The group differences were tested with the exact Wilcoxon test or paired *t* test. For exact Wilcoxon test, the *P* values from multiple comparisons within the same experiment were adjusted with the Bonferroni procedure.

Results

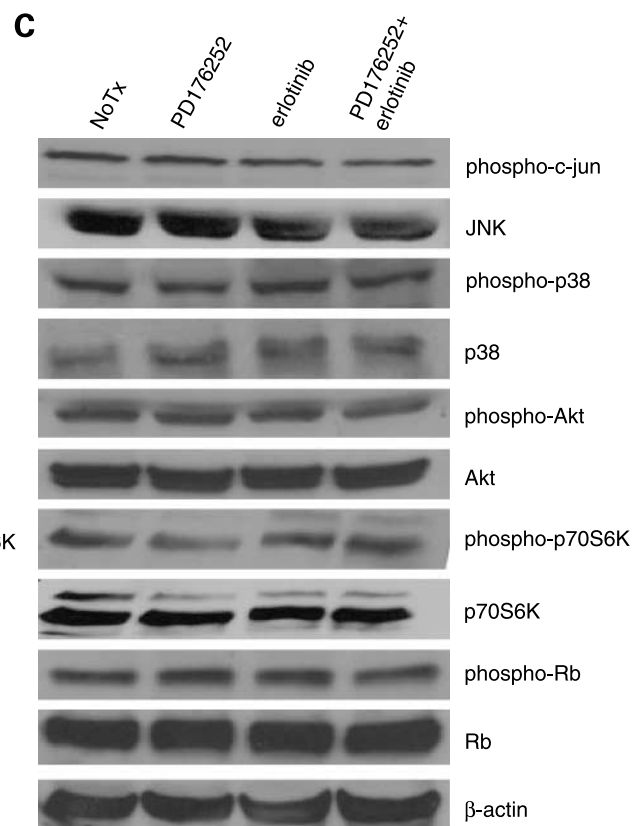
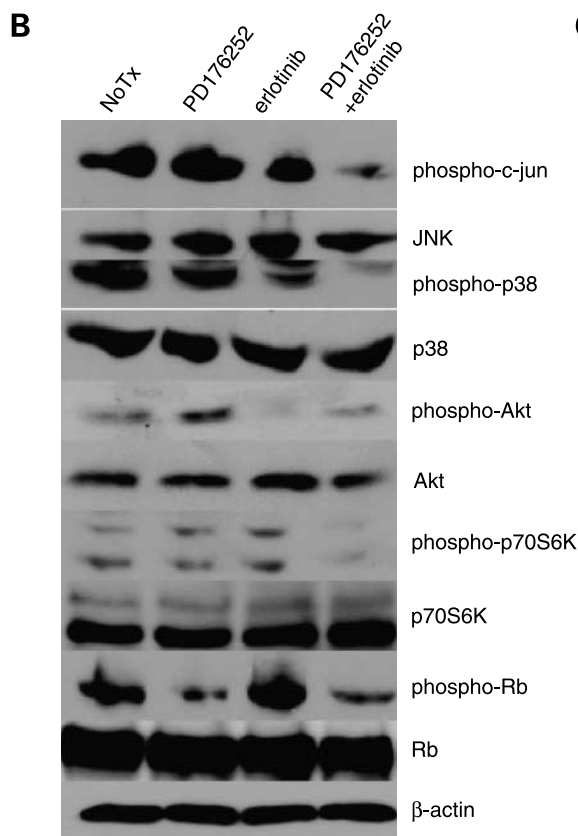
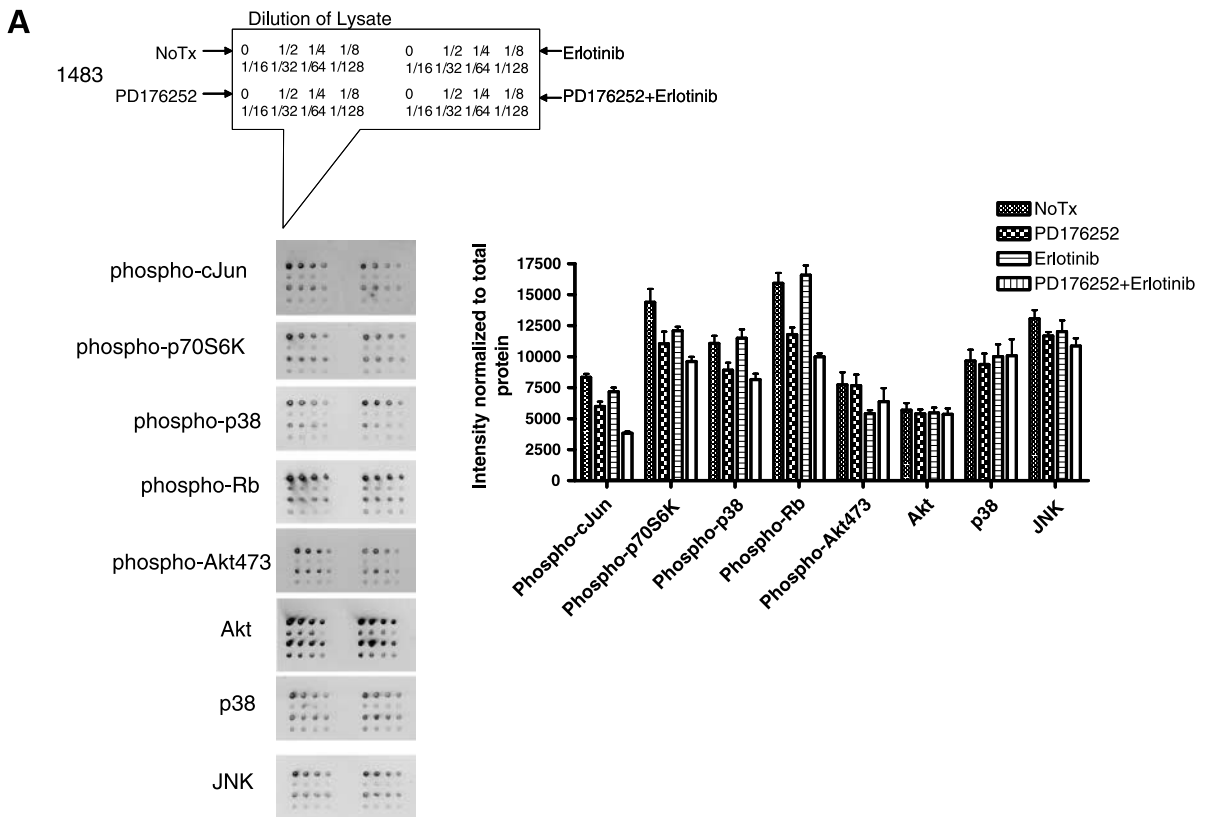
Inhibitory Effects of PD176252 and Erlotinib on Growth of HNSCC Cell Lines

We previously reported that inhibition of GRP using a neutralizing antibody 2A11 decreased HNSCC proliferation (24). EGFR inhibition has shown promise in clinical trials in HNSCC, especially when combined with irradiation (9, 25). To determine whether targeting GRPR and EGFR pathways in combination would enhance the therapeutic effects compared with either treatment alone, we compared several GRPR antagonists, 2A11, RC3940II, and PD176252 (17, 18, 26). For EGFR targeting, we examined the EGFR monoclonal antibody C225 and the EGFR tyrosine kinase

inhibitors erlotinib (Tarceva, OSI-774) and gefitinib (Iressa, ZD1839; refs. 8, 11). We optimized the combined targeting approach by comparing the relative growth inhibitory effects of the different combinations. The combination of the EGFR tyrosine kinase inhibitor erlotinib and the GRPR antagonist PD176252 showed the most reproducible effects *in vitro* (data not shown). As shown in Fig. 1A and B, in two HNSCC cell lines tested (UM-22B and 1483), both compounds inhibited HNSCC cell growth in a dose-dependent manner. The IC₅₀ for erlotinib ranged from 12 to 13 $\mu\text{mol/L}$ for UM-22B and 1483 cells, whereas the IC₅₀ for PD176252 was ~ 8 $\mu\text{mol/L}$ for both cell lines tested. These IC₅₀ values are consistent with previous reports using erlotinib or PD176252 in cancer cell lines (without EGFR activating mutations; refs. 27–30). In contrast, immortalized normal mucosal epithelial cells were relatively resistant to the growth inhibition by either of these agents. The IC₅₀ for erlotinib in HET-1A cells was 78 $\mu\text{mol/L}$, and for PD176252, the IC₅₀ value was 26 $\mu\text{mol/L}$ (Fig. 1C).

Combined Targeting of GRPR and EGFR Inhibits HNSCC, Cell Growth, Invasion, and Colony Formation

To test whether combined targeting of GRPR and EGFR resulted in enhanced growth inhibition compared with single treatment alone, half of the IC₅₀ dose for each drug was used to treat HNSCC cells followed by MTT assay. As shown in Fig. 2A and C, combined inhibition of both GRPR and EGFR resulted in significantly enhanced growth inhibition compared with either treatment alone over a 3-day treatment period ($P = 0.002$). In addition to half of the IC₅₀ dose, we tested additional lower concentrations to examine the effect of suboptimal doses on cytotoxicity. As shown in Fig. 2B, the same augmented inhibitory effects were observed using lower concentrations of the agents compared with either treatment alone ($P = 0.05$). We tested the antitumor effects of this compound in a xenograft model of HNSCC and found



that the tumors in the group of mice treated with a combination of erlotinib and PD176252 were significantly smaller than those mice treated with PD176252 alone ($P = 0.0475$; data not shown). However, PD176252 did relatively poorly *in vivo* and is not being further developed for clinical applications. To determine the potential toxicity of combined EGFR and GRPR inhibition on normal epithelial cells, the same treatment regimen was applied to an immortalized mucosal epithelial cell line (HET-1A). As shown in Fig. 2D, in contrast to the effects of the kinase inhibitors in HNSCC cells, the growth of the mucosal epithelial cells was not affected.

We previously reported that GRP induced HNSCC cell invasion (23). In addition to cell growth, the effects of combined EGFR and GRPR targeting in HNSCC cells on cell invasion were examined. As shown in Fig. 3A and B, although PD176252 or erlotinib alone decreased HNSCC cell invasion, combined targeting significantly enhanced the effect when compared with either treatment alone ($P < 0.001$).

To further investigate the potential therapeutic effect of GRPR and EGFR targeting on HNSCC progression, soft agar assays were used to determine colony formation from HNSCC cells. This assay can reflect the ability of a single cell to form a colony, which potentially reflects tumor progression (31). HNSCC cell colony-forming ability was further suppressed by combined treatment with PD176252 and erlotinib when compared with either treatment (Fig. 3C, $P < 0.001$).

Combined Targeting of GRPR and EGFR Increases HNSCC Apoptosis and G₁ Arrest

To determine whether the cytotoxic effects of combined EGFR and GRPR targeting were due to increased apoptosis and/or cell cycle alterations, we examined apoptosis by annexin V analysis following PD176252 and erlotinib treatment. As shown in Fig. 4A and B, combined targeting significantly enhanced HNSCC cell apoptosis at 24 h (Fig. 4A, $P = 0.008$; Fig. 4B, $P = 0.028$). In addition to annexin V analysis, similar results were also observed by terminal nucleotidyl transferase-mediated nick end labeling assay (data not shown). In contrast, treatment of HET-1A cells with PD176252, erlotinib, or PD176252 + erlotinib did not induce apoptosis compared with no treatment, although cisplatin was capable of robustly inducing apoptosis in these cells (Fig. 4C). Cell cycle analysis showed that combined treatment using PD176252 and erlotinib significantly induced G₁ arrest when compared with single treatment alone in 1483 cells (Table 1, $P = 0.028$). The cell cycle delay was also accompanied by a decreased percentage of S phase cells (Table 1, $P = 0.028$).

Combined Targeting of GRPR and EGFR Enhances Inhibition of HNSCC Signaling Pathways

To determine the molecular mechanism of combined inhibition of GRPR and EGFR, we investigated the effect of therapy on GRPR and EGFR signaling pathways. As shown in Fig. 5, combination targeting of GRPR and EGFR decreased EGFR phosphorylation levels compared with no treatment, but was not significantly different from erlotinib treatment alone, suggesting an EGFR-dependent effect. As a marker of proliferation, PCNA expression was further decreased upon combined targeting when compared with EGFR and GRPR inhibition alone ($P = 0.05$). MAPK phosphorylation was also decreased upon combined targeting of EGFR and GRPR when compared with GRPR targeting alone ($P = 0.05$). In addition, compared with either PD176252 or erlotinib treatment alone, combined GRPR and EGFR targeting increased PARP cleavage, a protein marker for cellular apoptosis ($P = 0.05$). These results suggest that combined therapy targeting EGFR and GRPR augments antitumor efficacy by inhibiting specific downstream signaling proteins.

Identification of Novel Markers that Are Regulated by Combined EGFR and GRPR Targeting

Enhanced antitumor effects were observed by combined GRPR and EGFR targeting, which indicates both EGFR-dependent and EGFR-independent pathways. We previously reported that secretion of both TGF- α and amphiregulin is induced by GRP in HNSCC cells (23, 32). To identify additional proteins that are regulated by GRPR and EGFR combined targeting, RPPA was used to analyze cell lysates from either PD176252, erlotinib, or PD176252 + erlotinib treatment. Using antibodies that specifically recognize the phosphorylated and total isoforms of kinase substrates, RPPA can multiplex and quantify a large array of activated proteins (33). Cell lysates were spotted on the nitrocellulose membrane and probed with 33 previously optimized phosphospecific and total antibodies to proteins involved in mitogenic signaling, signal transducing proteins, and transcription. To quantify the amount of proteins, cell lysates were diluted (1:2, 1:4, 1:8, 1:16, 1:32, 1:64, and 1:128). Using microvigene software, the amounts of corresponding proteins were determined. Quantitative results were obtained from four independent experiments and normalized to the levels of a panel of proteins that were relatively constant. As shown in Fig. 6A, combined treatment with PD176252 and erlotinib resulted in decreased levels of phosphorylated c-Jun compared with either treatment alone. To a lesser extent, phosphorylated p70S6K and p38 were down-regulated by treatment

Figure 6. Identification of novel markers that are regulated by EGFR and GRPR combined targeting by RPPA. **A**, 1483 cell lysates were harvested 3 d after PD176252 (4 $\mu\text{mol/L}$), erlotinib (6 $\mu\text{mol/L}$), or PD176252 + erlotinib treatment. Cell lysates were serially diluted followed by RPPA analysis with the antibodies indicated. One representative experiment is shown. The protein levels were quantitated by microvigene software. Cumulative results are shown from four independent experiments (*right*). **B**, the same 1483 cell lysates were subjected to immunoblotting with phospho-c-Jun, JNK, phospho-p38, P38, phospho-Akt (Ser⁴⁷³), Akt, phospho-p70S6K (Thr³⁸⁹), p70S6K, phospho-Rb (Ser^{807/811}), Rb, and β -actin to confirm the RPPA findings. **C**, HET-1A cell lysates were harvested 3 d after PD176252 (4 $\mu\text{mol/L}$), erlotinib (6 $\mu\text{mol/L}$), or PD176252 + erlotinib treatment. Cell lysates were subjected to immunoblotting with the antibodies used in **B**.

combined to either treatment alone. To confirm the RPPA results, the same cell lysates were subjected to immunoblotting with phosphospecific antibodies. As shown in Fig. 6B, phosphorylated c-Jun, p70S6K, and p38 levels were decreased upon combined targeting of GRPR and EGFR when compared with single treatment alone. Interestingly, phosphorylated Rb levels were decreased by the GRPR antagonist PD176252, but not by the EGFR inhibitor erlotinib. In contrast, phospho-Akt levels were decreased by erlotinib, but not by PD176252. Unlike HNSCC cells, the expression of downstream signaling proteins was not altered in HET-1A cells treated with erlotinib and/or PD176252 (Fig. 6C). These results suggest that the enhanced antitumor effects of combined targeting of GRPR and EGFR may be due to blockade of both EGFR-dependent as well as EGFR-independent pathways in HNSCC cells.

Discussion

The observation that elevated levels of growth factor receptors are associated with adverse cancer outcome has led to the development of approaches that specifically interrupt these autocrine pathways. Among them, EGFR monoclonal antibodies and EGFR tyrosine kinase inhibitors have been approved for use in cancer patients, including HNSCC.⁷ The administration of Erbitux/cetuximab/C225, in combination with radiation, has resulted in promising antitumor results compared with radiation alone (34). In addition to EGFR monoclonal antibodies, several different EGFR tyrosine kinase inhibitors have been used to treat cancer patients. These inhibitors compete with ATP binding to the tyrosine kinase domain of EGFR, which inhibits EGFR activity and blocks downstream signaling (35). OSI-774/Tarceva/erlotinib has been approved by the Food and Drug Administration for the treatment of non-small cell lung cancer (NSCLC). Erlotinib inhibits purified EGFR tyrosine kinase with an inhibitory concentration of 50% (IC₅₀) of 2 nmol/L. The kinase domains of the human insulin receptor and the insulinlike growth factor-I (IGF-I) receptor are much less sensitive to this inhibitor, and they are essentially unaffected at compound concentrations as high as 10 μmol/L. Erlotinib given p.o. or parenterally (i.p.) to mice consistently produced significant, dose-related reductions of EGFR tyrosine phosphorylation in HNSCC tumors (36). Despite these promising preclinical results, the response rates of HNSCC patients treated with EGFR inhibitors alone remains <10% (37).

We previously reported GRP/GRPR overexpression in head and neck tumors compared with normal mucosa, which inversely correlated with cancer patient survival (17). Studies have shown antitumor efficacy using GRPR-specific inhibitors in preclinical animal models (26, 38). A phase I clinical trial in lung cancer patients using a monoclonal antibody (2A11) against GRP showed no evidence of toxicity (39). Antitumor activity has been

observed with this anti-GRP antibody in patients with small cell lung cancer (40). PD176252, a nonpeptide GRPR ligand, significantly inhibited lung cancer growth *in vitro* and *in vivo* (30).

Here, we provide evidence of enhanced antitumor effects of GRPR and EGFR targeting strategies in head and neck cancer using the GRPR antagonist PD176252 and the EGFR tyrosine kinase inhibitor erlotinib. Combined inhibition of GRPR and EGFR additively inhibited HNSCC, but not normal mucosal epithelial cell proliferation. The decrease in viable tumor cells resulted from the induction of apoptosis, G₁ cell cycle arrest, and reduction of S phase. Although tumor cells often show signs of "oncogene addiction" to growth factor receptors, inhibition of the same receptors in normal cells may not affect cellular function(s). Thus, the increased IC₅₀ values of the EGFR and GRPR antagonists in the immortalized normal mucosal epithelial cells may be due to the lack of a requirement in these cells for EGFR or GRPR expression.

In addition to contributing to cell proliferation, we previously reported that Src family kinases, an important intermediate between GRPR and EGFR crosstalk, mediated GRP-induced HNSCC invasion (23). In the present study, we showed that combined targeting of GRPR and EGFR significantly inhibited cell invasion when compared with either treatment alone. These results indicate that by inhibiting Src activity both upstream and downstream of EGFR, cell invasion ability can be decreased by combined targeting of GRPR and EGFR. The effects on HNSCC cell growth by combined treatment could be the result of increased cell apoptosis and/or alterations in the cell cycle. Here, we showed that enhanced antitumor effects are due to increased cell apoptosis and G₁ cell cycle arrest. Using a clonogenic assay, combined targeting further inhibited colony formation when compared with single treatment, indicating the potential effects of combined targeting on HNSCC tumor progression, although it is unknown if our results in HNSCC cell lines can be generalized to the clinical setting.

Other GPCR inhibitors have also been used as antitumor agents. The bradykinin antagonist CU201 has been reported to produce additive or synergistic growth inhibition of lung cancer cell growth *in vitro* and *in vivo* when combined either with chemotherapy drugs or the EGFR inhibitor gefitinib (41). Targeting prostaglandin E₂ pathways using the cyclooxygenase-2 inhibitor celecoxib enhanced cell growth and colony formation inhibition, increased G₁ arrest, and apoptosis in head and neck cancer cells when combined with the EGFR inhibitor gefitinib (31). These findings suggest that combined targeting of GPCRs and EGFR may improve clinical outcome in cancer patients. However, the mechanisms responsible for the additive effects of targeting both GPCR and EGFR remain to be completely understood. If GPCR signaling acts predominantly through EGFR-dependent pathways, then EGFR targeting alone should achieve the same effect as combined targeting. The enhanced antitumor effects observed when targeting both receptors in combination suggests that EGFR-independent signaling pathways are also activated by GRP.

⁷ <http://www.fda.gov/cder/drug/infopage/erbitux/default.htm>

Using RPPA, we identified that several proteins that could potentially account for the enhanced antitumor effects of combinatorial targeting of GRPR and EGFR, including phospho-p70S6K, phospho-p38, and phospho-c-Jun. Phosphorylation of p70S6K by PDK1 or mTOR has been reported to stimulate translational initiation and contribute to cell growth (42, 43). We recently found that PDK1 serves as a key intermediate in the transactivation of EGFR by GRPR (32). With combined targeting of GRPR and EGFR, p70S6K activity may be affected by PDK1 and mTOR pathways. Phosphorylation of p38 has been reported to be directly activated by β -arrestin pathways and EGFR pathways (44, 45). Because β -arrestin acts downstream of GPCR pathways, combined inhibition of GRPR and EGFR can inhibit p38 activity via both EGFR-dependent and EGFR-independent pathways. Stimulation of GPCRs including GRPR has been reported to activate JNK and its signaling cascade. The activation of JNK by GRPR was shown to be dependent on Src and the $G\beta\gamma$ subunits and independent of phosphoinositide-3-kinase and EGFR signaling (46). As a transcription factor, c-Jun activity is affected by phosphorylation of p44/p42 MAPK as well as p38 MAPK (45, 47). Taken together, the expression of these phosphoproteins was affected by both EGFR-dependent and EGFR-independent pathways. In addition, we also identified Rb as a protein in which activity is regulated by GRPR, but not EGFR pathways. Rb regulates cell proliferation by controlling cell cycle progression from the G_1 -S phase. Here, we showed that PD176252 but not erlotinib decreased Rb phosphorylation, consistent with our cell cycle results (Table 1).

Accumulating evidence suggests that GPCR ligands activate EGFR and induce both proliferative and invasive pathways in cancer cells including HNSCC (17, 24, 48). Although some of the biological effects of these ligands seem to be mediated by EGFR, it is apparent that persistent activation of GPCR in the face of EGFR blockade contributes to tumor growth. Identification of the proteins that are induced by GRP, in the presence or absence of EGFR blockade, will determine the critical pathways to be targeted in combination with EGFR inhibition. The translational significance of these findings is underscored by our incomplete understanding of the mechanisms of "sensitivity" or "resistance" to EGFR inhibitors particularly in head and neck cancer, where recent studies support the therapeutic benefit of adding an EGFR inhibitor to standard therapy (49). Elucidation of the key pathways that are activated by GPCR ligands in the presence or absence of EGFR blockade will allow us to optimize therapeutic strategies that incorporate EGFR inhibition (alone or in combination with GPCR blockade) into cancer treatment regimens.

References

- Rogers SJ, Harrington KJ, Rhys-Evans P, O-Charoenrat P, Eccles SA. Biological significance of c-erbB family oncogenes in head and neck cancer. *Cancer Metastasis Rev* 2005;24:47–69.
- Ford AC, Grandis JR. Targeting epidermal growth factor receptor in head and neck cancer. *Head Neck* 2003;25:67–73.
- Drenning SD, Marcovitch AJ, Johnson DE, Melhem MF, Tweardy DJ, Grandis JR. Bcl-2 but not Bax expression is associated with apoptosis in normal and transformed squamous epithelium. *Clin Cancer Res* 1998;4:2913–21.
- Carvalho AL, Nishimoto IN, Califano JA, Kowalski LP. Trends in incidence and prognosis for head and neck cancer in the United States: a site-specific analysis of the SEER database. *Int J Cancer* 2005;114:806–16.
- Rubin Grandis J, Melhem MF, Gooding WE, et al. Levels of TGF- α and EGFR protein in head and neck squamous cell carcinoma and patient survival. *J Natl Cancer Inst* 1998;90:824–32.
- Rubin Grandis J, Chakraborty A, Melhem MF, Zeng Q, Tweardy DJ. Inhibition of epidermal growth factor receptor gene expression and function decreases proliferation of head and neck squamous carcinoma but not normal mucosal epithelial cells. *Oncogene* 1997;15:409–16.
- He Y, Zeng Q, Drenning SD, et al. Inhibition of human squamous cell carcinoma growth *in vivo* by epidermal growth factor receptor antisense RNA transcribed from the U6 promoter. *J Natl Cancer Inst* 1998;90:1080–7.
- Shin DM, Donato NJ, Perez-Soler R, et al. Epidermal growth factor receptor-targeted therapy with C225 and cisplatin in patients with head and neck cancer. *Clin Cancer Res* 2001;7:1204–13.
- Robert F, Ezekiel MP, Spencer SA, et al. Phase I study of anti-epidermal growth factor receptor antibody cetuximab in combination with radiation therapy in patients with advanced head and neck cancer. *J Clin Oncol* 2001;19:3234–43.
- Salomon DS, Brandt R, Ciardiello F, Normanno N. Epidermal growth factor-related peptides and their receptors in human malignancies. *Crit Rev Oncol Hematol* 1995;19:183–232.
- Baselga J. Targeting the epidermal growth factor receptor: a clinical reality. *J Clin Oncol* 2001;19:41–4S.
- Soulieres D, Senzer NN, Vokes EE, Hidalgo M, Agarwala SS, Siu LL. Multicenter phase II study of erlotinib, an oral epidermal growth factor receptor tyrosine kinase inhibitor, in patients with recurrent or metastatic squamous cell cancer of the head and neck. *J Clin Oncol* 2004;22:77–85.
- Fischer OM, Giordano S, Comoglio PM, Ullrich A. Reactive oxygen species mediate Met receptor transactivation by G protein-coupled receptors and the epidermal growth factor receptor in human carcinoma cells. *J Biol Chem* 2004;279:28970–8.
- Nilssen LS, Odegard J, Thoresen GH, Molven A, Sandnes D, Christoffersen T. G protein-coupled receptor agonist-stimulated expression of ATF3/LRF-1 and c-myc and comitogenic effects in hepatocytes do not require EGF receptor transactivation. *J Cell Physiol* 2004;201:349–58.
- Ueno Y, Sakurai H, Matsuo M, Choo MK, Koizumi K, Saiki I. Selective inhibition of TNF- α -induced activation of mitogen-activated protein kinases and metastatic activities by gefitinib. *Br J Cancer* 2005;92:1690–5.
- Lui V, Thomas SM, Zhang Q, et al. The mitogenic effects of gastrin-releasing peptide in head and neck squamous cancer cells are mediated by activation of the epidermal growth factor receptor. *Oncogene* 2003;22:6183–93.
- Lango MN, Dyer KF, Lui VW, et al. Gastrin-releasing peptide receptor-mediated autocrine growth in squamous cell carcinoma of the head and neck. *J Natl Cancer Inst* 2002;94:375–83.
- Ashwood V, Brownhill V, Higginbottom M, et al. PD 176252-the first high affinity non-peptide gastrin-releasing peptide (BB2) receptor antagonist. *Bioorg Med Chem Lett* 1998;8:2589–94.
- Pollack VA, Savage DM, Baker DA, et al. Inhibition of epidermal growth factor receptor-associated tyrosine phosphorylation in human carcinomas with CP-358,774: dynamics of receptor inhibition *in situ* and antitumor effects in athymic mice. *J Pharmacol Exp Ther* 1999;291:739–48.
- Sacks PG, Parnes SM, Gallick GE, et al. Establishment and characterization of two new squamous cell carcinoma cell lines derived from tumors of the head and neck. *Cancer Res* 1988;48:2858–66.
- Riser BL, Mitra R, Perry D, Dixit V, Varani J. Monocyte killing of human squamous epithelial cells: role for thrombospondin. *Cancer Res* 1989;49:6123–9.
- Stoner GD, Kaighn ME, Reddel RR, et al. Establishment and characterization of SV40 T-antigen immortalized human esophageal epithelial cells. *Cancer Res* 1991;51:365–71.
- Zhang Q, Thomas SM, Xi S, et al. SRC family kinases mediate epidermal growth factor receptor ligand cleavage, proliferation, and invasion of head and neck cancer cells. *Cancer Res* 2004;64:6166–73.

24. Lui VW, Thomas SM, Zhang Q, et al. Mitogenic effects of gastrin-releasing peptide in head and neck squamous cancer cells are mediated by activation of the epidermal growth factor receptor. *Oncogene* 2003;22:6183–93.
25. Bonner JA, Raisch KP, Trummell HQ, et al. Enhanced apoptosis with combination C225/radiation treatment serves as the impetus for clinical investigation in head and neck cancers. *J Clin Oncol* 2000;18:47–53S.
26. Kahan Z, Sun B, Schally AV, et al. Inhibition of growth of MDA-MB-468 estrogen-independent human breast carcinoma by bombesin/gastrin-releasing peptide antagonists RC-3095 and RC-3940-II. *Cancer* 2000;88:1384–92.
27. Sutter AP, Hopfner M, Huether A, Maaser K, Scherubl H. Targeting the epidermal growth factor receptor by erlotinib (Tarceva) for the treatment of esophageal cancer. *Int J Cancer* 2006;118:1814–22.
28. Dai Q, Ling YH, Lia M, et al. Enhanced sensitivity to the HER1/epidermal growth factor receptor tyrosine kinase inhibitor erlotinib hydrochloride in chemotherapy-resistant tumor cell lines. *Clin Cancer Res* 2005;11:1572–8.
29. Huang S, Armstrong EA, Benavente S, Chinnaiyan P, Harari PM. Dual-agent molecular targeting of the epidermal growth factor receptor (EGFR): combining anti-EGFR antibody with tyrosine kinase inhibitor. *Cancer Res* 2004;64:5355–62.
30. Moody TW, Leyton J, Garcia-Marin L, Jensen RT. Nonpeptide gastrin releasing peptide receptor antagonists inhibit the proliferation of lung cancer cells. *Eur J Pharmacol* 2003;474:21–9.
31. Chen Z, Zhang X, Li M, et al. Simultaneously targeting epidermal growth factor receptor tyrosine kinase and cyclooxygenase-2, an efficient approach to inhibition of squamous cell carcinoma of the head and neck. *Clin Cancer Res* 2004;10:5930–9.
32. Zhang Q, Thomas SM, Lui VW, et al. Phosphorylation of TNF- α converting enzyme by gastrin-releasing peptide induces amphiregulin release and EGF receptor activation. *Proc Natl Acad Sci U S A* 2006;103:6901–6.
33. Sheehan KM, Calvert VS, Kay EW, et al. Use of reverse phase protein microarrays and reference standard development for molecular network analysis of metastatic ovarian carcinoma. *Mol Cell Proteomics* 2005;4:346–55.
34. Bonner JA, Harari PM, Giralt J, et al. Radiotherapy plus cetuximab for squamous-cell carcinoma of the head and neck. *N Engl J Med* 2006;354:567–78.
35. Arteaga CL, Baselga J. Tyrosine kinase inhibitors: why does the current process of clinical development not apply to them? *Cancer Cell* 2004;5:525–31.
36. Easty DM, Easty GC, Carter RL, Monaghan P, Butler LJ. Ten human carcinoma cell lines derived from squamous carcinomas of the head and neck. *Br J Cancer* 1981;43:772–85.
37. Baselga J, Trigo JM, Bourhis J, et al. Phase II multicenter study of the antiepidermal growth factor receptor monoclonal antibody cetuximab in combination with platinum-based chemotherapy in patients with platinum-refractory metastatic and/or recurrent squamous cell carcinoma of the head and neck. *J Clin Oncol* 2005;23:5568–77.
38. Miyazaki M, Lamharzi N, Schally AV, et al. Inhibition of growth of MDA-MB-231 human breast cancer xenografts in nude mice by bombesin/gastrin-releasing peptide (GRP) antagonists RC-3940-II and RC-3095. *Eur J Cancer* 1998;34:710–7.
39. Chaudhry A, Carrasquillo JA, Avis IL, et al. Phase I and imaging trial of a monoclonal antibody directed against gastrin-releasing peptide in patients with lung cancer. *Clin Cancer Res* 1999;5:3385–93.
40. Kelley MJ, Linnoila RI, Avis IL, et al. Antitumor activity of a monoclonal antibody directed against gastrin-releasing peptide in patients with small cell lung cancer. *Chest* 1997;112:256–61.
41. Chan DC, Gera L, Stewart JM, et al. Bradykinin antagonist dimer, CU201, inhibits the growth of human lung cancer cell lines *in vitro* and *in vivo* and produces synergistic growth inhibition in combination with other antitumor agents. *Clin Cancer Res* 2002;8:1280–7.
42. Brown EJ, Beal PA, Keith CT, Chen J, Shin TB, Schreiber SL. Control of p70 s6 kinase by kinase activity of FRAP *in vivo*. *Nature* 1995;377:441–6.
43. Podsypanina K, Lee RT, Politis C, et al. An inhibitor of mTOR reduces neoplasia and normalizes p70/S6 kinase activity in Pten \pm mice. *Proc Natl Acad Sci U S A* 2001;98:10320–5.
44. Sun Y, Cheng Z, Ma L, Pei G. β -Arrestin 2 is critically involved in CXCR4-mediated chemotaxis, and this is mediated by its enhancement of p38 MAPK activation. *J Biol Chem* 2002;277:49212–9.
45. Lefkowitz RJ, Shenoy SK. Transduction of receptor signals by β -arrestins. *Science* 2005;308:512–7.
46. Chan AS, Wong YH. Gq-mediated activation of c-Jun N-terminal kinase by the gastrin-releasing peptide-preferring bombesin receptor is inhibited upon costimulation of the Gs-coupled dopamine D1 receptor in COS-7 cells. *Mol Pharmacol* 2005;68:1354–64.
47. Weston CR, Lambright DG, Davis RJ. Signal transduction. MAP kinase signaling specificity. *Science* 2002;296:2345–7.
48. Gschwind A, Prenzel N, Ullrich A. Lysophosphatidic acid-induced squamous cell carcinoma cell proliferation and motility involves epidermal growth factor receptor signal transactivation. *Cancer Res* 2002;62:6329–36.
49. Bonner JA, Giralt J, Harari PM, et al. Cetuximab prolongs survival in patients with locoregionally advanced squamous cell carcinoma of head and neck: a phase III study of high dose radiation therapy with or without cetuximab [abstract no 5507]. *Am Soc Clin Oncol* 2004.

Molecular Cancer Therapeutics

Antitumor mechanisms of combined gastrin-releasing peptide receptor and epidermal growth factor receptor targeting in head and neck cancer

Qing Zhang, Neil E. Bhola, Vivian Wai Yan Lui, et al.

Mol Cancer Ther 2007;6:1414-1424.

Updated version Access the most recent version of this article at:
<http://mct.aacrjournals.org/content/6/4/1414>

Cited articles This article cites 48 articles, 24 of which you can access for free at:
<http://mct.aacrjournals.org/content/6/4/1414.full#ref-list-1>

Citing articles This article has been cited by 9 HighWire-hosted articles. Access the articles at:
<http://mct.aacrjournals.org/content/6/4/1414.full#related-urls>

E-mail alerts [Sign up to receive free email-alerts](#) related to this article or journal.

Reprints and Subscriptions To order reprints of this article or to subscribe to the journal, contact the AACR Publications Department at pubs@aacr.org.

Permissions To request permission to re-use all or part of this article, use this link
<http://mct.aacrjournals.org/content/6/4/1414>.
Click on "Request Permissions" which will take you to the Copyright Clearance Center's (CCC) Rightslink site.